2010

Residential Heat Pump Heating Performance with Single Faults Imposed

William Vance Payne
National Institute of Standards and Technology

Seok Ho Yoon
Korea Institute of Machinery and Materials

Piotr A. Domanski
National Institute of Standards and Technology

Residential Heat Pump Heating Performance with Single Faults Imposed

Seok Ho Yoon[1], W. Vance Payne[2*], Piotr A. Domanski[2]

[1] Department of Energy Plant, Korea Institute of Machinery and Materials
Daejeon 305-343, KOREA
shyoon@kimm.re.kr

[2] Building and Fire Research Laboratory, National Institute of Standards and Technology
Gaithersburg, MD 20899-8631, USA
301-975-6663, vance.payne@nist.gov

* Corresponding Author

ABSTRACT

A heat pump equipped with a thermostatic expansion valve (TXV) was tested in environmental chambers during steady-state no-fault and imposed-fault operation. The studied system was an R410A split residential heat pump with an 8.8 kW nominal cooling capacity, Seasonal Energy Efficiency Ratio (SEER) of 13, and Heating Seasonal Performance Factor (HSPF) of 7.8. The imposed faults were compressor valve leakage, outdoor improper air flow, indoor improper air flow, liquid line restriction, refrigerant undercharge, and refrigerant overcharge. Evaporator fouling, condenser fouling, and refrigerant overcharge caused the greatest performance degradation. We observed substantial commonality between sensitive features in the heating and cooling modes; however, several different features were identified for the heating mode as more sensitive.

Keywords: fault detection and diagnosis; heating mode; heat pump; thermostatic expansion valve

1. INTRODUCTION

Improvements in electronics and sensors, and an increasing interest in energy saving in buildings have given an impetus for fault detection and diagnostics (FDD) research for space conditioning and refrigeration equipment. Among several studies published in the nineties, Stylianou and Nikanpour (1996) represented a methodology using thermodynamic modeling, pattern recognition, and expert knowledge to determine the health of a reciprocating chiller and to diagnose selected faults. Rossi and Braun (1997) developed a statistical FDD method for a roof-top air conditioner. The FDD system was operated with seven representative temperature measurements. Statistical properties of the residuals for current and normal operation were used to classify the current operation as faulty or normal. Five types of faults could be distinguished from their diagnosis. Breuker and Braun (1998) surveyed frequently occurring faults for a packaged air conditioner using field data. Li (2004) re-examined the statistical rule-based method initially formulated by Rossi and Braun (1997) and presented two additional FDD schemes which improved the sensitivity of the FDD module. He also provided virtual sensors to estimate characteristic parameters from indirect component modeling. Li and Braun (2007) examined a large amount of data to determine general features for any vapor compression system that clearly indicated a particular fault regardless of load level. This "decoupling" technique was shown to produce accurate indications of individual system faults even in the presence of multiple and simultaneous faults. However, only a few cases of FDD studies for heat pumps have been implemented. Kim et al. (2008) investigated the performance of a residential heat pump operating in the cooling mode. This paper reports on basic FDD measurements on an 8.8 kW air-to-air heat pump operated in the heating mode under fault-free conditions and with single faults imposed.

2. EXPERIMENTAL SETUP

2.1 System Description and Implementation of Faults

The studied system was an R410A, 8.8 kW (2.5 ton), split residential heat pump (Figure 1) with Seasonal Energy Efficiency Ratio (SEER) of 13 and Heating Seasonal Performance Factor (HSPF) of 7.8 (AHRI, 2008). The unit was comprised of the indoor fan-coil section, outdoor section with a scroll compressor, thermostatic expansion valves (TXV's), and connecting tubing. Table 1 lists the faults studied, and detailed specifications of the test rig including indoor ductwork, dimensions, data acquisition and instrumentations were described in Kim et al. (2006).

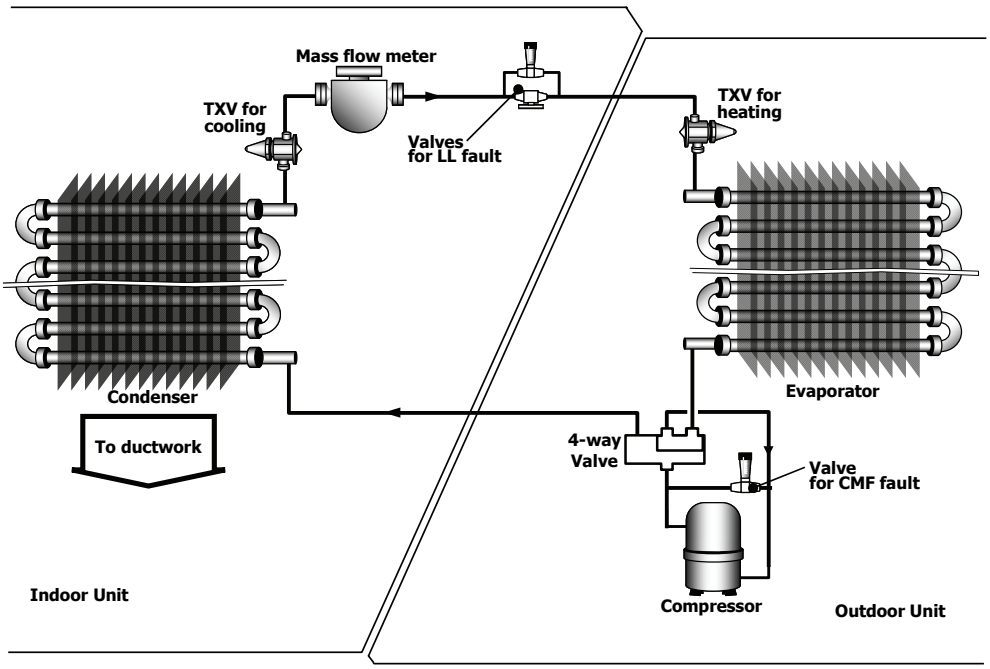

Figure 1: Experimental setup with the heat pump in the heating mode

Table 1: Description of studied faults

Fault	Abbreviation	Determination of fault level during tests
Compressor/4-way valve leakage	CMF	% of refrigerant flow rate
Improper outdoor air flow rate	EF	% of coil area blocked
Improper indoor air flow rate	CF	% of air flow rate reduction
Liquid line restriction	LL	% of normal pressure drop through liquid line
Refrigerant overcharge	OC	% overcharge from the correct charge
Refrigerant undercharge	UC	% undercharge from the correct charge

2.2 Experimental Procedure and Test Conditions

A comprehensive test series was carried out to map the performance of the system at normal (fault-free) operation and with imposed faults. Table 2 presents operating conditions for the test program. The test schedule for fault-free steady-state operation involved all 13 listed test conditions, where test 1 and test 2 were the AHRI Standard 210/240 tests. With the exception of tests 1 and 2, the outdoor humidity was low enough to ensure a dry outdoor coil; imposing faults while frosting was occurring was not considered due to the unpredictable nature of frost formation. For all tests, the indoor relative humidity was controlled roughly around 50 % since moisture is not an influential parameter for performance of the condenser. The faulty tests were performed at two conditions indicated in Table 2 by two asterisks (tests 4 and 10). Only two outdoor temperatures were used because cooling mode tests have shown linearity in faulty performance characteristics with changes in evaporator temperature (Kim et. al. 2006).

Table 2: Operating conditions for all tests

Test index	Indoor		Outdoor	
	Dry-bulb temp. (ºC)	Relative humidity (%)	Dry-bulb temp. (ºC)	Relative humidity (%)
1*	21.1	40~60	-8.3	70
2*	21.1	40~60	8.3	73
3	15.6	40~60	-8.3	dry coil
4**	21.1	40~60	-8.3	dry coil
5	23.9	40~60	-8.3	dry coil
6	15.6	40~60	1.7	dry coil
7	21.1	40~60	1.7	dry coil
8	23.9	40~60	1.7	dry coil
9	15.6	40~60	8.3	dry coil
10**	21.1	40~60	8.3	dry coil
11	23.9	40~60	8.3	dry coil
12	21.1	40~60	16.7	dry coil
13	23.9	40~60	16.7	dry coil

1* Low temperature heating condition from AHRI standard
2* High temperature heating condition from AHRI standard
** Test conditions selected for fault tests.

3. TEST RESULTS

3.1 Fault-Free Test Results

Figure 2 presents variation of selected system features and performance parameters at different operating conditions with respect to outdoor dry-bulb temperature. Refrigerant superheat T_{sh} shows a minimum (Figure 2(a)) while refrigerant subcooling T_{sc} increases linearly as the outdoor temperature decreases (Figure 2(b)). The heating capacity Q_{AIR} shows a linear change with outdoor dry-bulb temperature and no influence of indoor dry-bulb temperature (Figure 2(c)). COP show a nearly perfectly linear variation with respect to the outdoor and indoor dry-bulb temperature in Figure 2(d), which implies also a linear variation of the compressor power.

3.2 Performance Variation with Single Faults

The feature residuals were calculated using the definition as shown in Equation (1). The reference value, $\phi_{i,\text{reference}}$, was the measured value from the fault-free steady-state testing.

$$\mathrm{R}(\phi_i) = \phi_{i,\text{measurements}} - \phi_{i,\text{reference}} \tag{1}$$

3.2.1 Compressor/reversing valve leakage: The compressor/reversing valve leakage fault (CMF) involved at least three fault levels. The fault level was calculated as the ratio of refrigerant mass flow through the system with the fault imposed divided by the refrigerant mass flow rate during fault-free operation.

Compressor leakage causes a reduction in refrigerant mass flow rate, as shown in Figure 3(a). It also demonstrates itself in a decrease in refrigerant superheat T_{sh}, condenser saturation temperature T_C, and condenser air temperature rise ΔT_{CA} (Figure 3). Capacity and COP are also degraded.

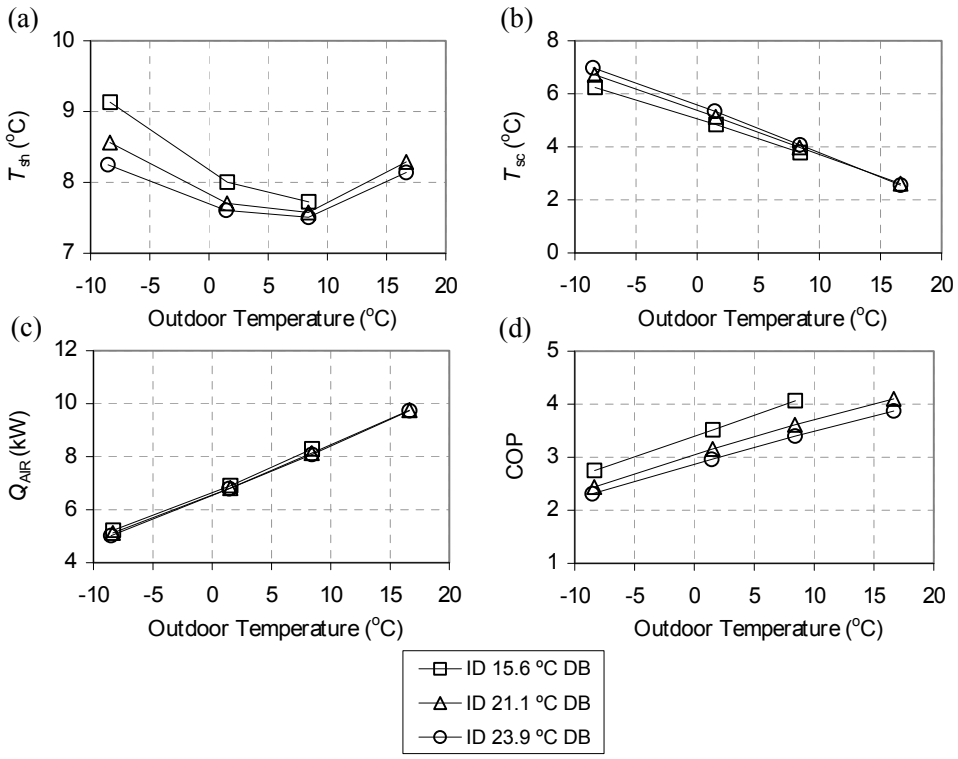

Figure 2: Variation of system performance under fault-free condition; (a) T_{sh}, (b) T_{sc}, (c) Q_{AIR}, (d) COP

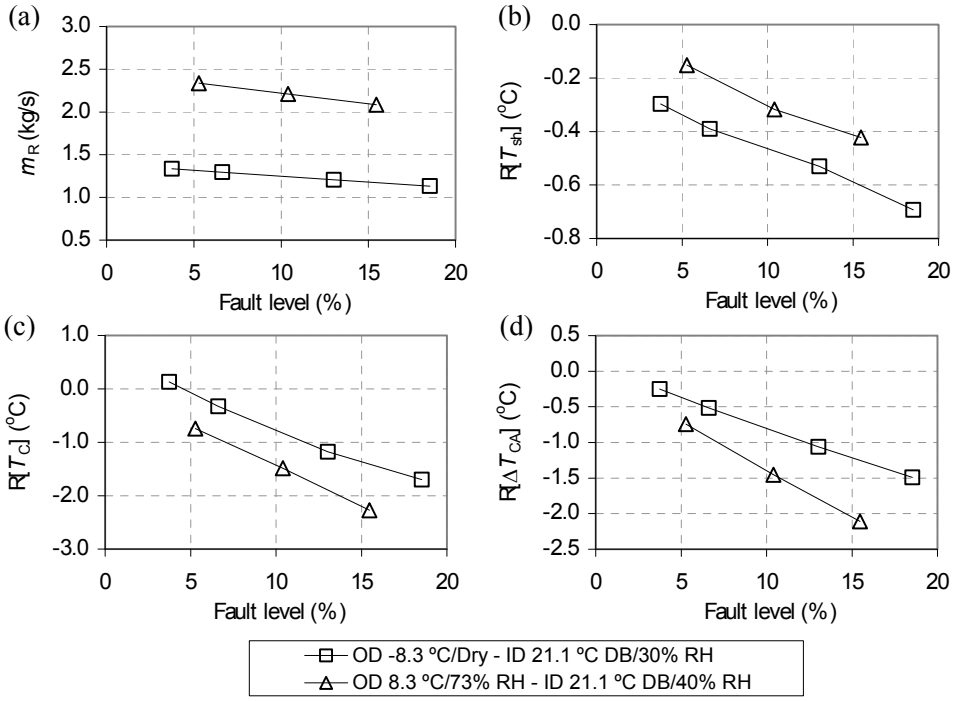

Figure 3: Variation of system parameters at the compressor/reversing valve leakage fault; (a) m_R, (b) Residual of T_{sh}, (c) Residual of T_C, (d) Residual of ΔT_{CA}

3.2.2 Improper indoor air flow rate (condenser fouling): The improper indoor air flow rate fault was implemented by controlling the speed of the nozzle chamber booster fan located at the end of the ductwork. Reducing the indoor air flow (increasing external static pressure) approximates fouling. The tests included three fault levels at approximately 10 %, 20 %, and 30 %, which corresponded to respective reductions of the air flow rate from the no-fault condition. The reduction of air flow rate increased T_C (Figure 4(a)) and T_D (Figure 4(c)), which increased compressor work W_{comp} (Figure 4(d)). The influence of improper air flow rate through the condenser on the evaporator temperature T_E was small (Figure 4(b)).

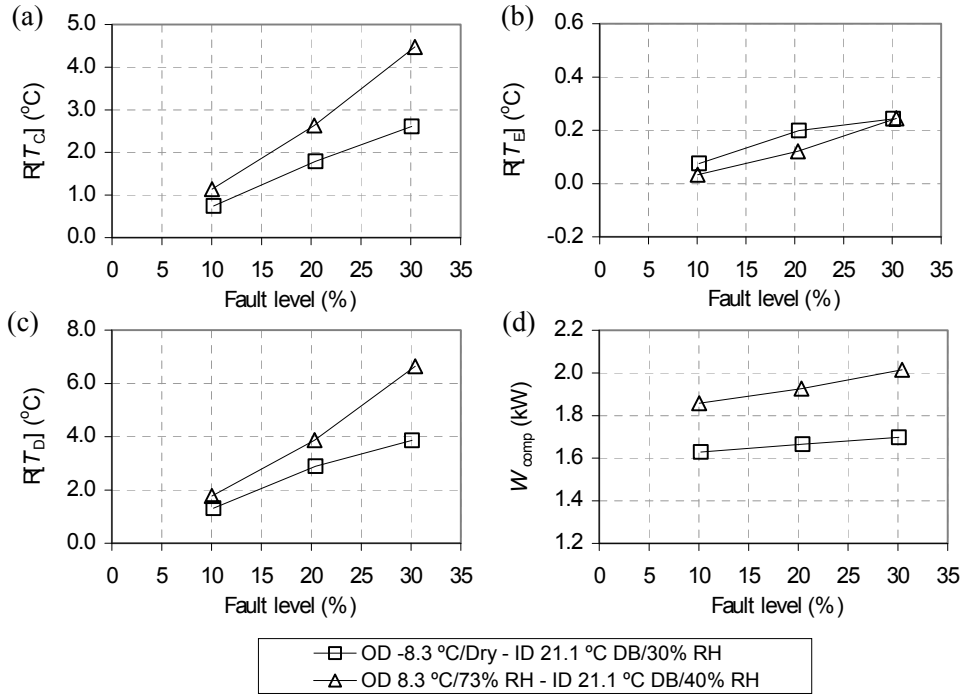

Figure 4: Variation of system parameters with improper indoor coil air flow rate fault: (a) Residual of T_C, (b) Residual of T_E, (c) Residual of T_D, (d) W_{comp}

3.2.3 Liquid line restriction: The liquid line restriction fault was implemented by modulating the settings of two valves, as seen in Figure 1, installed in parallel in the liquid line. The liquid line restriction fault level was numerically assigned by the ratio of the increase in the liquid line pressure drop with respect to the no-fault condition. The LL fault level varied up to 50 %, above which we were concerned about compressor damage. As seen in Figure 5, a 50 % liquid line restriction fault was very difficult to detect using superheat or subcooling. It seems that the TXV could adjust refrigerant mass flow rate even when the liquid line pressure drop increased by 50 %. The liquid line restriction does not reduce capacity and COP significantly.

3.2.4 Improper outdoor air flow rate (evaporator fouling): Fault levels of 10 %, 20 %, and 30 % were implemented by blocking the corresponding percentage of the finned frontal area of the outdoor coil beginning at the bottom of the heat exchanger. Since the outdoor unit is installed in an open space this fault may be caused by newspaper, grass, debris, blowing snow, etc. As the heat transfer area of the evaporator was reduced, evaporator temperature T_E decreased (Figure 6(a)) lowering suction vapor density and refrigerant mass flow rate (Figure 6(b)). Consequently, liquid subcooling T_{sc} increased (Figure 6(c)) and compressor work W_{comp} decreased (Figure 6(d)).

3.2.5 Refrigerant undercharge and overcharge: The fault level for refrigerant undercharge and refrigerant overcharge was calculated as the ratio of the charge deviation from the refrigerant charge set according to manufacturer's specifications in the cooling mode. The test program included six fault levels: ±10 %, ±20 %, and ±30 %, where negative and positive signs represent undercharge and overcharge, respectively. A combination of residuals for T_{sh}, T_{sc}, and T_C provides an indication of refrigerant undercharge or overcharge for a 10 % fault (Figure 7(a,b,c)).

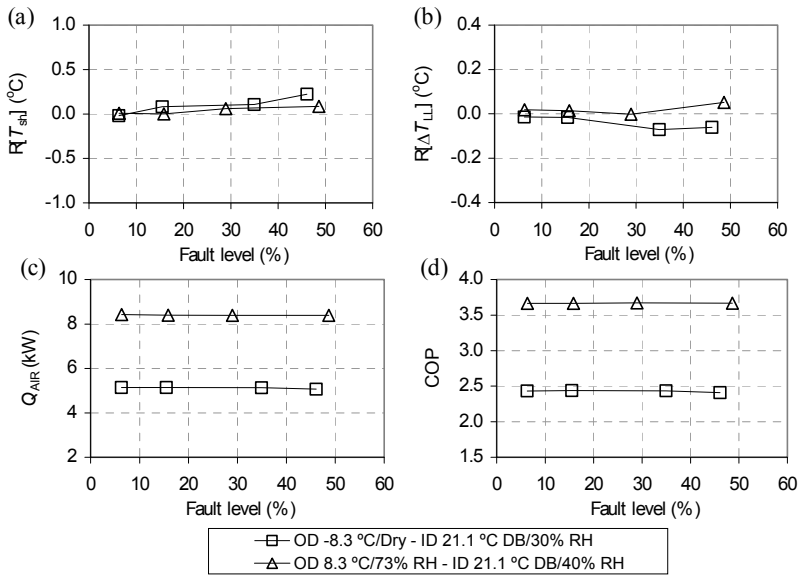

Figure 5: Variation of system parameters for the liquid line restriction fault: (a) Residual of T_{sh}, (b) Residual of ΔT_{LL}, (c) Q_{AIR}, and (d) COP

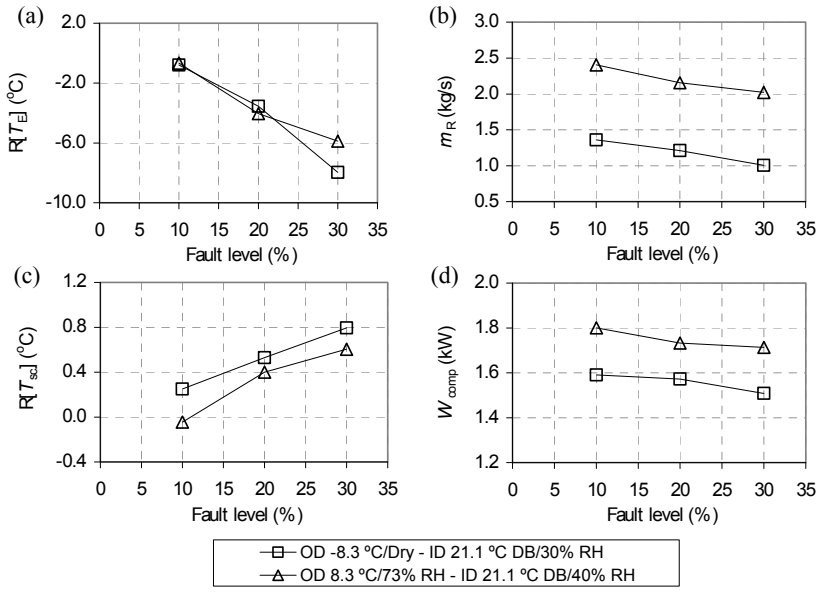

Figure 6: Variation of system parameters with improper outdoor coil (evaporator) air flow rate fault: (a) Residual of T_E, (b) Residual of m_R, (c) Residual of T_{sc}, (d) W_{comp}

An overcharge increased the compressor suction pressure causing an increase in refrigerant suction density, increase in refrigerant mass flow rate, which in turn produced an increased refrigerant subcooling at the expansion device inlet. Test results show that the maximum COP occurred at 10 % refrigerant undercharge (Figure 7(d)). This is a result of the refrigerant charge being optimized for the cooling mode.

3.3 Fault Level Effect on Performance Degradation

Figure 8 compares the degradation of capacity and COP for the different faults as a function of fault level. Liquid line restriction had almost no effect on capacity and COP at up to a 30 % fault level and was the least discernible fault in this study. Refrigerant overcharge also had a small effect on capacity, which somewhat increased with

increasing fault level, but the COP decreased. The other faults degraded the COP at a similar rate while degrading the capacity to a different degree. Evaporator fouling had the greatest affect upon capacity.

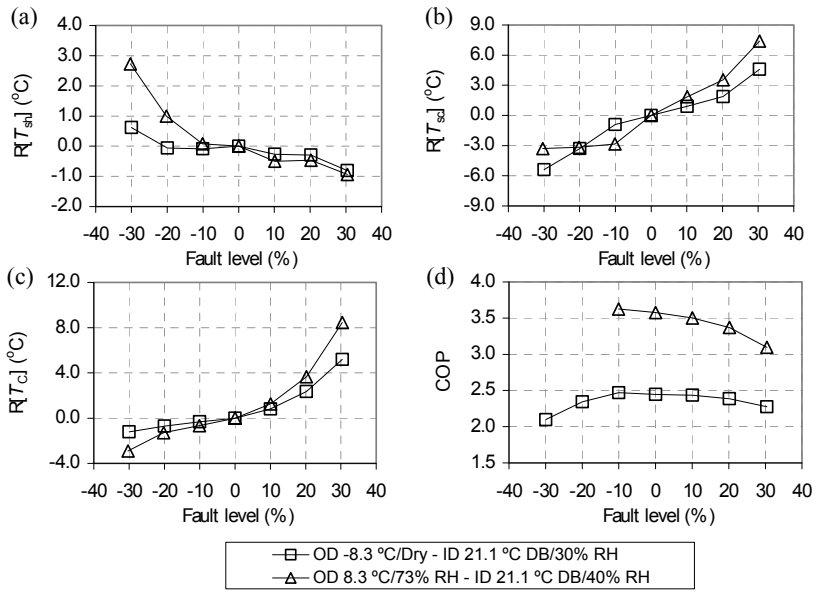

Figure 7: Variation of system parameters at the improper refrigerant charge fault: (a) Residual of T_{sh}, (b) Residual of T_{sc}, (c) Residual of T_C, (d) COP

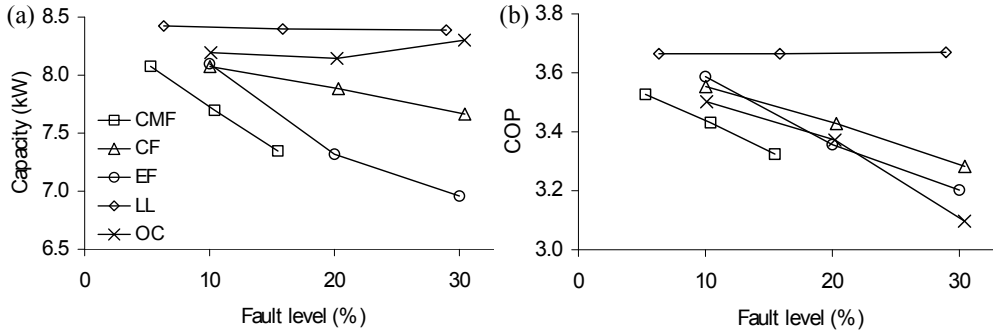

Figure 8: Performance degradation with regard to fault level (8.3 ºC outdoor dry-bulb temperature, 74 % relative humidity, and 21.1 ºC indoor dry-bulb temperature): (a) Capacity, (b) COP

4. SENSITIVE FEATURES FOR HEATING VERSUS COOLING

Table 3 compares the most sensitive features for heating and cooling for each fault identified in this study and the previous study by Kim et al. (2006). The table shows substantial similarities; however, some differences can be noticed. The most noticeable difference in fault effects is the very minimal sensitivity of the heat pump, operating in the heating mode, to liquid line restriction even for very high fault levels.

5. CONLCUDING REMARKS

The paper presents basic FDD data for a TXV-equipped heat pump operating in the heating mode. Overcharge, evaporator fouling, and condenser fouling caused the greatest performance degradation. The laboratory data are limited to frost-free operation because of unpredictable system behavior during outdoor heat exchanger frost formation. Consequently, the envisioned diagnostic scheme will be limited to frost-free operation. While current defrost boards have become sophisticated, the sensors used for fault detection can further improve defrost performance. We observed substantial commonality between sensitive features in the heating and cooling modes; however, several different features were identified for the heating mode as being more sensitive.

Table 3: Most sensitive features for the single faults imposed

Fault	Feature for heating	Feature for cooling	Comment
Compressor/Reversing Valve Leakage	T_C, ΔT_{CA}	T_C, T_E	
Condenser Air flow	T_C, T_D, ΔT_{CA}	T_{sc}, T_D, T_C	
Evaporator Air flow	T_E, T_C, ΔT_{CA}	T_E, ΔT_{EA}	
Liquid Line Restriction	-	T_{sh}, ΔT_{LL}, T_D	TXV mitigates this fault
Refrigerant Undercharge	T_{sc}, ΔT_{CA}	T_{sc}, T_{sh}, T_D	COP more affected by undercharge
Refrigerant Overcharge	T_{sc}, T_C, T_D	T_{sc}, T_D, T_C	

NOMENCLATURE

CF	condenser air flow fault	(-)	T_C	condenser inlet saturation temperature	T_C
CMF	compressor/reversing valve leakage fault	(-)	T_D	compressor discharge-line wall temperature	(°C)
COP	coefficient of performance	(-)	T_E	evaporator exit saturation temperature	(°C)
DB	dry-bulb temperature		ΔT_{CA}	condenser air temperature rise	(°C)
EF	evaporator air flow fault	(-)	ΔT_{EA}	evaporator air temperature drop	(°C)
ID	indoor		ΔT_{LL}	liquid line temperature drop	(°C)
LL	refrigerant liquid line restriction fault	(-)	T_{sc}	liquid line subcooling	(°C)
m_R	refrigerant mass flow rate	(kg/s)	T_{sh}	evaporator exit superheat	(°C)
OC	refrigerant overcharge fault	(-)	UC	refrigerant undercharge fault	(°C)
OD	outdoor		W_{comp}	compressor work	(kW)
Q_{AIR}	condenser air-side capacity	(kW)			
R	residual of features	(-)		**Greek Symbol**	
RH	relative humidity		ϕ	feature or performance parameter	

REFERENCES

AHRI Standard 210/240-2008, "Performance Rating of Unitary Air-Conditioning and Air-Source Heat Pump Equipment," Air Conditioning, Heating, and Refrigeration Institute, Arlington, VA. www.ahrinet.org

Breuker, M.S. and Braun, J.E., 1998, "Common faults and their impacts for rooftop air conditioners," *International Journal of Heating, Ventilating, Air-Conditioning and Refrigerating Research*, 4(3), 303-18.

Kim, M., Payne, W.V., Domanski, P.A., and Hermes, C.J.L, 2006, "Performance of a residential heat pump operating in the cooling mode with single faults imposed," NISTIR 7350, NIST, Gaithersburg, MD, USA. http://www.bfrl.nist.gov/863/HVAC/pubs/2006%20Building%20Publications%20-%20NISTIR_7350.htm

Kim, M., Yoon, S. H., Payne, W. V., and Domanski, P. A., 2008, "Design of a steady-state detector for fault detection and diagnosis of a residential air conditioner," *International Journal of Refrigeration*, Vol. 31, No. 5, pp. 790-799.

Li H., 2004, A decoupling-based unified fault detection and diagnosis approach for packaged air conditioners. Ph.D. Thesis, West Lafayette, IN: Purdue University.

Li, H. and Braun, J.E., 2007, "Decoupling features and virtual sensors for diagnosis of faults in vapor compression air conditioners", *International Journal of Refrigeration,* 30, 546-64.

Rossi, T.M. and Braun, J.E., 1997, "A Statistical, Rule-based Fault Detection and Diagnostic Method for Vapor Compression Air Conditioners," *HVAC&R Research*, Vol. 3, No. 1, pp. 19-37.

Stylianou, M. and Nikanpour, D., 1996, "Performance Monitoring, Fault Detection, and Diagnosis of Reciprocating Chillers," *ASHRAE Transactions*, Vol. 102, Part 1, pp. 615-627.